Pulsed ultrasound modulated optical tomography utilizing the harmonic response of lock-in detection

H. Ruan, M. L. Mather, and S. P. Morgan*

Electrical Systems and Optics Research Division, Faculty of Engineering, University of Nottingham,
University Park, Nottingham NG7 2RD, UK

*Corresponding author: steve.morgan@nottingham.ac.uk

Ultrasound modulated optical tomography (USMOT) can image the optical properties of a scattering medium at a spatial resolution approaching that of ultrasound (US). A lock-in parallel speckle detection technique is proposed to detect pulsed US modulated light using a multipixel detector. The frequency components of the pass band match those of the US pulse train and provide efficient detection. The modulation depth is extracted by taking the difference between a pair of speckle patterns modulated by a pair of phase-inversed US bursts. Modification to pulse inversion mode enables the second harmonic US modulation due to nonlinear US propagation to be detected.   © 2013 Optical Society of America

OCIS codes: (110.6150) Speckle imaging; (110.0113) Imaging through turbid media.
http://dx.doi.org/10.1364/AO.52.004755

1. Introduction

Ultrasound modulated optical tomography (USMOT) is a hybrid imaging technique used to image heavily optically scattering media. In tissue imaging, USMOT has the potential to provide the functional information, e.g., blood oxygenation saturation, of optical techniques at a spatial resolution approaching that of ultrasound (US). The technique involves applying both light and focused US to a scattering medium. Light that passes through the US column becomes modulated by the US (often called optical tagging). This produces a modulated optical speckle pattern at the detector, which provides localized information about the optical properties in this region.

Leveque and co-workers introduced a parallel lock-in detection method [1,2] which was used to extract the modulated intensity of the detected speckle at each pixel in a detector array. In this method, the scattered light in the US focal zone is modulated

at the frequency of the US and the light source is turned on for either the 1st, 2nd, 3rd, or 4th quarter of the modulation period. By combining the intensities measured during these quarters, detection analogous to a lock-in amplifier can be achieved, allowing high frequency signals to be demodulated (∼MHz) by a low frame rate detector (∼Hz). A simplified version showed that comparable performance could be achieved using two- or three-phase steps [3]. To date, this method has only been applied for continuous wave (CW) US.

Analogous to conventional US imaging, improved axial resolution can be achieved by pulsing the US and time gating the detection. As demodulation techniques are often optimized for single-frequency CW detection, energy is lost when wideband US pulses are applied. Lev and Sfez [4] developed a method which used short (4 cycles) US bursts to achieve high axial resolution while also maintaining narrow band detection. Individual pulses were recorded using a fast detector and an analog to digital converter, and the phase of the pulses was conserved between pulses. Stitching these phase-conserved pulses

together produces a narrow band signal and improves signal-to-noise ratio (SNR) over the wideband case. As this method requires the shape of the US modulated pulse to be recorded directly to allow pulse reshaping, it is not compatible with a parallel lock-in approach using a CCD camera. Narrow band filtering detection methods such as Fabry–Perot interferometer detection [5], holography [6,7], and spectral hole burning [8] also encounter problems in dealing with wide band US pulses, as modulated signals are filtered out. Often, US tone bursts that are several cycles long are used [6,8] in order achieve a compromise between matching the signal bandwidth to the filter bandwidth and obtaining high axial resolution. As an alternative to filter-based approaches, speckle contrast detection with intense acoustic bursts [9] has been used to detect a wide bandwidth modulated signal; however, this approach is also sensitive to wide bandwidth noise and, for nonlinear imaging, cannot completely separate the fundamental and second harmonic US modulated signals.

For the first time to our knowledge, we present a phase stepping method that can efficiently demodulate pulsed USMOT signals which have a high harmonic content due to using a train of US pulses. By utilizing short-pulsed optical illumination synchronized to a train of US pulses an optical speckle pattern is obtained within the integration time of the detector. In the next camera frame, the train of US pulses is inverted and another speckle pattern is acquired. Combining these two speckle patterns provides a pass band which allows detection of the harmonic components of the US modulated optical signal. It should be noted that the harmonic components referred to here are at the pulse repetition frequency and not due to nonlinear propagation of the US. It is also interesting to note that in conventional lock-in detection, the objective is to avoid detection of harmonic components, but here we make use of this property to improve performance. By simple modification of the pulse sequence, the pass band of the detection can be modified to detect the second harmonic USMOT signal due to nonlinear propagation of the US. This method involves using a train of alternating inverted and noninverted US pulses to obtain a speckle pattern within the detector integration time. Shifting this sequence by $\pi/2$ in the next camera frame and then combining the speckle patterns enables the second harmonic signal to be extracted.

2. Theory

Figure 1 shows the principle of the method for extracting optical modulation by US with linear propagation. A pair of phase-inversed, single-cycle US bursts [Figs. 1(a) and 1(b)] is used to modulate the strobed laser illumination [Fig. 1(c)], which is synchronized with US pulses arriving at the focal zone of the US transducer. At the detector, an optical speckle pattern with intensities fluctuating over the
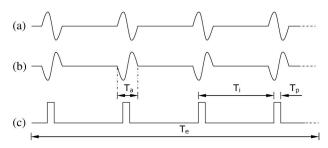

Fig. 1. Single cycle US arriving at the US focal zone after delay; (a) 0 phase frame; (b) π phase frame; (c) synchronized laser pulses (T_a, US pulse duration; T_i, interval time between pulses; T_p, laser pulse duration; T_e, camera exposure time).

same range of frequencies as the US is produced. Over the camera exposure time, the pixels collect thousands of laser pulses (typically ∼2000, 50 ns duration, 50 μs interval time, 100 ms exposure time) corresponding to the same phase of the US pulse [Fig. 1(a)]. The same process then repeats for the next frame but modulated by US pulses with the inverse phase [Fig. 1(b)]. Taking the difference of the two speckle patterns obtained in consecutive frames cancels the common unmodulated signal while the modulated signal remains. Although the overall bandwidth of the detected optical pulses is wide, consisting of a fundamental and multiple harmonics with $1/T_i$ frequency interval (where T_i is the interval time between pulses), each frequency component has a corresponding inverted counterpart which results in narrow band detection of each harmonic component of the modulated pulse.

To analyze the spectra of the US pulse trains, the time series of single cycle sinusoidal US bursts separated by a time interval T_i [Fig. 1(a)] is represented as a Fourier series

$$S_0(t) = \sum_{n=1}^{\infty} A_n \cos(n\omega_0 t) + B_n \sin(n\omega_0 t), \quad (1)$$

where

$$A_n = \frac{1}{2\pi}\left[\frac{1}{b/a + n} + \frac{1}{b/a - n}\right]\left[1 - \cos\left(2\pi n \frac{a}{b}\right)\right];$$

$$B_n = -\frac{1}{2\pi}\left[\frac{1}{b/a + n} + \frac{1}{b/a - n}\right]\sin\left(2\pi n \frac{a}{b}\right);$$

$\omega_0 = 2\pi/T_i$; T_i is the interval time between pulses; a/b is the duty cycle of the single cycle tone burst; n, a, b are integers.

Similarly, the tone burst sequence with inverted phase is represented as

$$S_1(t) = \sum_{n=1}^{\infty} A_n \cos(n\omega_0 t + \pi) + B_n \sin(n\omega_0 t + \pi). \quad (2)$$

From Eqs. (1) and (2), it can be seen that each frequency component has a phase-inversed

counterpart. Considering a single frequency component, which has a pair of inverted pulses associated with it, this method is similar to the two-phase CW parallel lock-in method [3], in which the US modulation of the laser is shifted by π to enable phase stepping. Following this method, the US modulation depth M can be obtained,

$$M = \frac{\sqrt{\langle(I_{0,i} - I_{1,i})^2\rangle/2}}{\langle(I_{0,i} + I_{1,i})/2\rangle}, \tag{3}$$

where $I_{0,i}$ and $I_{1,i}$ are the values recorded on the ith pixel of frame 0 (0 phase modulation) and frame 1 (π phase modulation) respectively; $\langle\cdot\rangle$ denotes averaging over the detected speckle pattern. Extending this to all frequency components in the US pulse results in each harmonic component being demodulated. It should be noted that Eq. (3) is a simplified derivation which ignores the integration time of the camera. A more rigorous derivation has been carried out previously for the CW case [2] and, for completeness in the Appendix, we have derived the AC intensity for the optical signal modulated by the fundamental (linear propagation) US. However it should be noted that, apart from some constant scaling factors, the numerator in Eq. (3) is not substantially different to Eq. (A12) and therefore the simplified method used here is valid.

To analyze the power spectra of the US pulse trains, simulated 0 and π phase US burst sequences are generated for a 2.25 MHz single cycle tone burst with a 100 kHz repetition rate and a laser pulse length of 111 ns, parameters which are also used in the experiments. The power spectra of the sequences are identical and so only one spectrum is shown in Fig. 2(a). There are discrete frequency components at nf_1, where $f_1 = 100$ kHz. The envelope of the spectrum is given by the Fourier coefficients A_n and B_n as

described in Eq. (1) and is related to the US pulse duration. The bandwidth of each frequency component is inversely proportional to the overall length of the tone burst sequence which is defined by the camera exposure time. For example, for a 10 ms exposure time, an individual frequency bandwidth is 100 Hz, resulting in $Q = 1000$ at $f_1 = 100$ kHz, where the Q factor is the ratio of the central frequency and pass bandwidth.

To analyze the pass band of the lock-in detection, the laser pulse train is also simulated. As the laser pulses are synchronized with the US bursts, the detection response has frequency components at the same discrete frequencies nf_1 as the US spectrum. The envelope of the detection response is a sinc function whose width is inversely proportional to the laser pulse duration T_a. The laser pulse width should be small enough to allow wide band US bursts to pass. Figures 2(b) and 2(c) show examples at laser pulse durations of 111 and 360 ns, respectively. As the individual frequency components of the lock-in detection method are precisely matched to those of the modulated signal, the harmonic components of the wideband US modulated signal can be detected while wideband noise can be filtered out efficiently.

This method can also be adapted to detect the second harmonic US modulation due to nonlinear acoustic wave propagation, which can be used to improve spatial resolution and reduce side lobes [10,11]. It should be noted that the term "harmonic" here indicates the signal generated by the nonlinear acoustic wave propagation and not the harmonics introduced by modulating the light with an US pulse discussed previously. The second harmonic signal generation depends on the nonlinear coefficient of the medium and the propagation distance, and significantly increases as the US pressure becomes higher. To detect the second harmonic signal due to nonlinear US propagation efficiently, a pulse inversion technique [10] has also been developed to overcome the problem of overlapping bands when wide-bandwidth US pulses are used. In this technique, a pair of phase-inverted US pulses is detected and then summed, resulting in the fundamental signal cancelling out while maintaining the second harmonic.

To apply the parallel lock-in technique to second harmonic USMOT signals, the US pulse train [Fig. 1(a)] is modified to a series of pulses in which each pulse is phase inverted to the previous one within the same camera exposure time (Fig. 3). During the camera exposure period, the laser pulses are modulated by multiple pairs of phase-inverted US pulses, resulting in the fundamental modulated signal cancelling out and the second harmonic signal, due to nonlinear US propagation, being detected [Fig. 3(a)]. The resulting speckle pattern is the first image of the two-phase, lock-in parallel speckle detection algorithm. To obtain the second speckle image due to second harmonic modulation, the US at the fundamental frequency is shifted by $\pi/2$ which
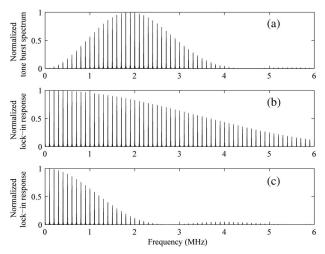

Fig. 2. Simulated data, (a) power spectrum of the sequence of US bursts with pulse frequency 2.25 MHz, repetition rate 100 kHz; (b) lock-in detection harmonic response with 111 ns laser pulse duration, 100 kHz repetition rate; (c) same as (b) but with a pulse duration of 360 ns.
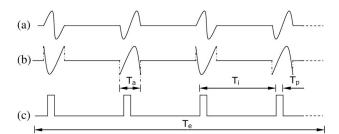
Fig. 3. Single cycle US arriving at the US focal zone after delay; (a) $0 - \pi$ phase frame; (b) $\pi/2 - 3\pi/2$ phase frame; (c) synchronized laser pulses.

produces a π phase shift at the second harmonic frequency [Fig. 3(b)] [10]. The second harmonic US modulation depth is obtained by processing these two speckle images following the algorithm described in Eq. (3).

The pass band of the lock-in detection for the second harmonic is similar to that used for detecting the fundamental signal and is shown in Fig. 4(a), with its zoom in version in Fig. 4(b). The difference between harmonics due to nonlinear US propagation and harmonics due to applying a short US pulse can be clearly observed in Fig. 4(c). The spectrum due to modulation as a result of linear propagation of US has a higher magnitude and is centered at the fundamental frequency that due to modulation by nonlinear US propagation is of lower magnitude and is centred at the second harmonic frequency. Each spectrum has an associated set of harmonic components at the pulse repetition frequency. In conventional US, the two spectra overlap; however, upon closer inspection of the discrete frequency bands [Fig. 4(d)] it can be seen that in this case they are well separated. The frequency components of the second harmonic modulation signal [highlighted by the dashed vertical lines in Fig. 4(d)] are precisely matched to the second
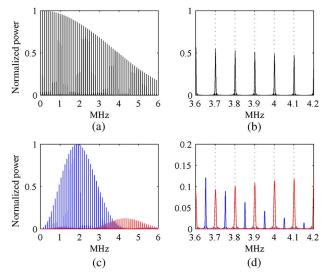

Fig. 4. (a) Pass band of the lock-in detection; (b) zoom in version of (a); (c) power spectra of the nonlinear US pulse train showing fundamental (left-hand side) and second harmonic (right-hand side); (d) zoom in version of (c). The dashed vertical lines in (b) and (d) indicate the second harmonic components.

harmonic lock-in response obtained by pulse inversion parallel lock-in detection [Fig. 4(b)].

3. Experiment

In the experimental setup (Fig. 5), a 2.25 MHz, 48 mm focal length US transducer [Olympus A304S, 17 mm focal zone length, 1.83 mm measured full-width half-maximum (FWHM) lateral beamwidth at focus] is driven by single-cycle sinusoidal tone bursts with $T_i = 45$ μs time interval (generated by a Tektronix AFG3252 function generator and amplified by an ENI A300 RF power amplifier). When the US pulse reaches the transducer focal point (after $T_d = 32$ μs in this case), a laser diode with a variable pulse duration (Sanyo DL-6148-030, 638 nm wavelength, 40 mW power, Thorlabs LTC100-B driver) strobes the scattering medium at the US modulation corresponding to either 0 or π phase (or 0 and $\pi/2$ for second harmonic imaging). A CCD camera (Hamamatsu ORCA C4742-95-12ERG, 1344 × 1024 pixels, 12 bits, pixel size 6.45 μm × 6.45 μm) is placed 10 cm behind a 5 mm diameter aperture to ensure approximately 4 pixels per speckle [12]. Two consecutive speckle pattern images modulated by phase-inversed tone bursts are recorded by the camera using a 180 ms exposure time for each. Implementing Eq. (3) and scanning the sample enables an image of the modulation depth to be obtained. Including frame transfer and processing times, the acquisition time for each pair of speckle patterns is ~800 ms for both fundamental and second harmonic detection. Averaging the signal 10 times is carried out to reduce noise. For additional validation of the shape of the US pulses, a needle hydrophone (Precision Acoustics, 0.2 mm) was used to measure the pulsed US pressure at four phases.

In an experiment to investigate US modulation at the fundamental frequency, four optically absorbing objects were embedded at the mid-plane of an 18 mm thick agarose phantom mixed with microspheres (scattering coefficient $\mu_s = 3.0$ mm^{-1}, anisotropy factor $g = 0.938$, no additional absorption added). The absorbing objects [Fig. 6(a)] are 3 mm × 2 mm with 3 mm spacing in the x dimension and 2 mm spacing in the y dimension, and are obtained by printing onto a transparent film (polyester, 100 μm thick). In order to maintain constant optical and acoustic properties in the region of interest, the scattering medium was raster scanned on the x–y plane along with a 0.4 mm
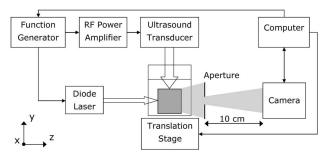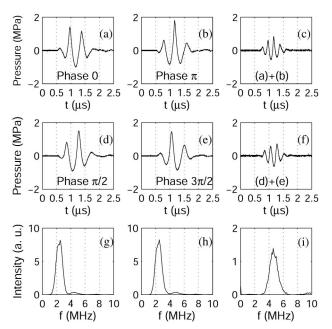

Fig. 5. System setup.

Fig. 6. Measured US pulses at four phases and the corresponding spectra. (a) Phase 0; (b) phase π; (c) sum of (a) and (b); (d) phase $\pi/2$; (e) $3\pi/2$; (f) sum of (d) and (e); (g)–(i) spectra of (a)–(c).

step size. In order to quantify the lateral resolution improvement by detecting the second harmonic US modulated signal, a pair of pulse inversion US pulse trains [10] was used in the same system to image an optically absorbing edge embedded at the mid-plane of a scattering gel (16 mm thick, $\mu_s = 2.4$ mm^{-1}). This sample is slightly more weakly scattering than that used in the previous experiment as the second harmonic component is smaller (by a factor of ~0.2) than the fundamental.

4. Results

Figures 6(a) and 6(b) show the US pulses measured with a needle hydrophone at phase 0 and phase π. Compared with Fig. 3(a), some additional ringing appears in the measured waveform, but the fundamental signals are similarly inverted as shown in Figs. 6(a) and 6(b). Figure 6(c) shows the summation

of Figs. 6(a) and 6(b), in which the fundamental frequency is cancelled while the second harmonic component remains. The $\pi/2$ shifted pulses [Fig. 3(b)] were also measured and shown in Figs. 6(d) and 6(e), with their sum shown in Fig. 6(f). The second harmonic signals are inverted as shown in Figs. 6(c) and 6(f). Figures 6(g)–6(i) show the spectra of Figs. 6(a)–6(c). Compared with the spectrum profile of the ideal pulse train [Fig. 4(c)], the measured spectra are narrower as the transducer acts as a band pass filter but Fig. 6(c) demonstrates rejection of the fundamental signal.

At each step, both the US modulated signal [AC signal, Eq. (3)] and mean light intensity on the CCD (DC signal) were detected. The AC image [Fig. 7(b)] shows that the absorbing objects are discernible whereas they cannot be resolved in the DC image [Fig. 7(c)].

The results of the line scan of the edge embedded within a scattering medium is shown in Fig. 8(a); the rising edge of the scan is sharper with second harmonic signal detection than that with fundamental signal detection. This edge response function can be used to estimate the line spread function by a least squares fitting of an inverse polynomial, which is a rational approximation of the integral of Gaussian function [13]. Figure 8(b) shows the line spread functions with FWHM of 9.26 mm (DC), 4.02 mm (fundamental), and 2.43 mm (second harmonic), respectively.

5. Discussion and Conclusion

The pulsed US modulated optical signals are broadband but consist of a series of discrete harmonic frequencies at the pulse repetition frequency. The signals can be detected by matching the pass band of the lock-in detection to that of the pulsed US modulated signal. Using a sequence of pulses (0 phase) followed by an inverted sequence (π phase), the background optical speckle is suppressed while the modulated signal is enhanced. The axial image resolution can be improved by using higher-frequency US pulses and an appropriate laser pulse width. Moreover, by using pulse inversion US pulse
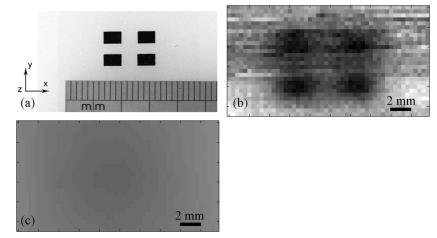

Fig. 7. (a) Objects embedded into the scattering gel; (b) image of pulsed US modulation (AC image); (c) light intensity image (DC image).
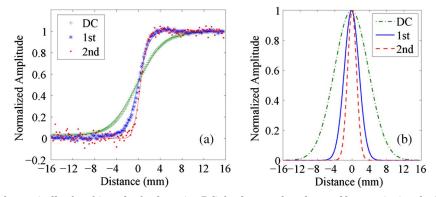
Fig. 8. (a) Line scans of an optically absorbing edge by detecting DC, fundamental, and second harmonic signals. (b) Line spread functions based on the fitting to the edge response functions; FWHM are 9.26 mm (DC), 4.02 mm (fundamental), and 2.43 mm (second harmonic).

trains, the nonlinear second harmonic and fundamental US modulated signals are well separated. By detecting the nonlinear second harmonic US modulated optical signals, the lateral resolution of USMOT imaging can also be improved [10]. To allow sufficient light to be detected, the exposure time to acquire each speckle pattern is set to 180 ms, which is much longer than the optical speckle decorrelation time of many tissues in vivo. However, this harmonic lock-in detection technique can be further revised and combined with holography techniques [6] which can effectively reduce the speckle decorrelation effect.

As shown in Fig. 2, different filter responses can be obtained by varying the laser pulse duration length, and this can be used to optimize the SNR. An example is obtained from the US modulated signal spectrum shown in Fig. 2(a). This example assumes that the modulation depth = 10^{-6} and that the detection is shot noise limited by the DC light level, producing white noise proportional to the square root of the DC light level. As the intended application area for such techniques is in tissue imaging, we also assume that we are limited by the average optical and ultrasonic intensity to comply with safety regulations. Therefore when the pulse duration is shorter, the peak intensity rises accordingly to maintain a constant average intensity.

Passing both the signal spectrum and noise spectrum through a range of filters corresponding to different pulse durations [such as those shown in Figs. 2(b) and 2(c)] allows the SNR for a range of pulse durations to be obtained. As shown in Fig. 9, shorter pulses provide better performance due to the increase in peak optical intensity matched to a corresponding increase in US intensity over the same time period.

It is also interesting to compare the performance of this demodulation method with conventional detection of pulsed and CW US modulated optical signals. The CW case follows a similar analysis that was carried out for optimizing the laser pulse duration. Ensuring that the average optical and US signals match those of the pulsed case and the laser pulse duration is 1/4 of the US wavelength [2], the SNR of the CW case is ~57. This is a factor of ~5 lower

than the optimized results shown in Fig. 9 for the pulsed case. Although the CW case has a narrower detection bandwidth, the improvement in SNR is because both the synchronized US and optical peak intensities are higher and the resulting US modulated signal is proportional to the product of these intensities [14].

There are also, of course, practical drawbacks with using CW US, as time gated detection cannot be performed along the acoustic axis, thus limiting its application.

In conclusion, the lock-in parallel speckle detection technique can detect pulsed US modulated light using a multipixel detector. The frequency components of the pass band match those of the US pulse train and provide efficient detection. The modulation depth is extracted by taking the difference between a pair of speckle patterns modulated by a pair of phase-inversed US bursts. Modification to pulse inversion mode enables the second harmonic US modulation due to nonlinear US propagation to be detected. The multipixel detection of optical signals modulated by pulsed US provides a useful approach for enabling time gating along the acoustic axis and optimizing SNR.
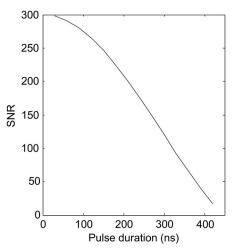

Fig. 9. SNR for different laser pulse durations for the signal spectrum shown in Fig. 2(a). A modulation depth = 10^{-6} and shot noise limited detection is assumed.

Appendix A

Here we show a more rigorous derivation of the modulated light intensity that takes into account the finite integration time of the detector. This is similar to the derivation previously carried out for the CW case [2] but generalizes this to an arbitrary duty cycle of the optical pulse being modulated by an US pulse train.

The laser pulse train (modulation function) is given by

$$D(t) = \frac{a}{b} + \sum_{n=1}^{\infty} C_n \, \cos(\omega_0 n t), \qquad (A1)$$

where

$$C_n = \frac{2}{n\pi} \, \sin\left(\frac{\omega_0 n a}{2}\right)$$

is the Fourier coefficient.

Let $I(t)$ be the light intensity on each pixel of the camera if the laser intensity were kept constant as described in [2].

$$I(t) = I_{\text{dc}} + I_{\text{ac}} S_0'(t, \varphi), \qquad (A2)$$

where

$$S_0'(t, \varphi) = \sum_{n=1}^{\infty} A_n \, \cos(n\omega_0 t + \varphi) + B_n \, \sin(n\omega_0 t + \varphi),$$

and φ is the random phase of the speckle.

Multiplying by the modulation function and integrating over the exposure time of the detector, the intensity on ith pixel for the first US pulse train is given by

$$I_{0,i} = \int_0^{T_e} I(t) D(t) \mathrm{d}t, \qquad (A3)$$

$$I_{0,i} = \int_0^{T_e} [I_{\text{dc}} + I_{\text{ac}} S_0'(t, \varphi)] \left[\frac{a}{b} + \sum_{n=1}^{\infty} C_n \, \cos(\omega_0 n t)\right] \mathrm{d}t, \qquad (A4)$$

$$I_{0,i} = I_{\text{dc}} \frac{a}{b} T_e + \int_0^{T_e} \left[I_{\text{ac}} S_0'(t, \varphi) \sum_{n=1}^{\infty} C_n \, \cos(\omega_0 n t)\right] \mathrm{d}t, \qquad (A5)$$

$$I_{0,i} = I_{\text{dc}} \frac{a}{b} T_e + I_{\text{ac}} \int_0^{T_e} \sum_{m=1}^{\infty} \sum_{n=1}^{\infty} C_m \, \cos(m\omega_0 t)$$
$$\times [A_n \, \cos(n\omega_0 t + \varphi) + B_n \, \sin(n\omega_0 t + \varphi)] \mathrm{d}t, \qquad (A6)$$

$$I_{0,i} = I_{\text{dc}} \frac{a}{b} T_e$$
$$+ I_{\text{ac}} \int_0^{T_e} \sum_{n=1}^{\infty} [A_n C_n \times \cos(n\omega_0 t) \cos(n\omega_0 t + \varphi)$$
$$+ B_n C_n \times \cos(n\omega_0 t) \sin(n\omega_0 t + \varphi)] \mathrm{d}t, \qquad (A7)$$

$$I_{0,i} = I_{\text{dc}} \frac{a}{b} T_e + \frac{I_{\text{ac}}}{2} T_e \sum_{n=1}^{\infty} [A_n C_n \, \cos(\varphi) + B_n C_n \, \sin(\varphi)]. \qquad (A8)$$

In order to demodulate I_{ac}, another speckle pattern $I_{1,i}$ with phase-inverted US modulation is captured,

$$I_{1,i} = I_{\text{dc}} \frac{a}{b} T_e - \frac{I_{\text{ac}}}{2} T_e \sum_{n=1}^{\infty} [A_n C_n \, \cos(\varphi) + B_n C_n \, \sin(\varphi)]. \qquad (A9)$$

Taking the difference of these frames,

$$I_{0,i} - I_{1,i} = I_{\text{ac}} T_e \sum_{n=1}^{\infty} [A_n C_n \, \cos(\varphi) + B_n C_n \, \sin(\varphi)], \qquad (A10)$$

$$\langle (I_{0,i} - I_{1,i})^2 \rangle = \frac{1}{2} I_{\text{ac}}^2 T_e^2 \left[\left(\sum_{n=1}^{\infty} A_n C_n\right)^2 + \left(\sum_{n=1}^{\infty} B_n C_n\right)^2\right], \qquad (A11)$$

where $\langle \cdot \rangle$ denotes average over all the pixels. It should be noted that T_e, A_n, B_n, and C_n are constants. Rearranging (A11), we have

$$I_{\text{ac}} \propto \sqrt{\langle (I_{0,i} - I_{1,i})^2 \rangle}. \qquad (A12)$$

Therefore, the simplified Eq. (3) is applicable in the pulsed US modulation case and is applied in this system.

References

1. S. Leveque, A. C. Boccara, M. Lebec, and H. Saint-Jalmes, "Ultrasonic tagging of photon paths in scattering media: parallel speckle modulation processing," Opt. Lett. **24**, 181–183 (1999).
2. S. Leveque-Fort, "Three-dimensional acoustic-optic imaging in biological tissues with parallel signal processing," Appl. Opt. **40**, 1029–1036 (2000).
3. J. Li and L. V. Wang, "Methods for parallel-detection-based ultrasound-modulated optical tomography," Appl. Opt. **41** 2079–2084 (2002).
4. A. Lev and B. G. Sfez, "Pulsed ultrasound-modulated light tomography," Opt. Lett. **28**, 1549–1551 (2003).
5. S. Sakadzic and L. V. Wang, "High-resolution ultrasound-modulated optical tomography in biological tissues," Opt. Lett. **29**, 2770–2772 (2004).
6. M. Atlan, B. C. Forget, F. Ramaz, A. C. Boccara, and M. Gross, "Pulsed acousto-optic imaging in dynamic scattering media with heterodyne parallel speckle detection," Opt. Lett. **30**, 1360–1362 (2005).

7. L. Sui, R. A. Roy, C. A. DiMarzio, and T. W. Murray, "Imaging in diffuse media with pulsed-ultrasound-modulated light and the photorefractive effect," Appl. Opt. **44**, 4041–4048 (2005).

8. Y. Li, H. Zhang, C. Kim, K. H. Wagner, P. Hemmer, and L. V. Wang, "Pulsed ultrasound-modulated optical tomography using spectral-hole burning as a narrowband spectral filter," Appl. Phys. Lett. **93**, 011111 (2008).

9. R. J. Zemp, C. Kim, and L. V. Wang, "Ultrasound-modulated optical tomography with intense acoustic bursts," Appl. Opt. **46**, 1615–1623 (2007).

10. H. Ruan, M. L. Mather, and S. P. Morgan, "Pulse inversion ultrasound modulated optical tomography," Opt. Lett. **37**, 1658–1660 (2012).

11. B. Ward, A. C. Baker, and V. F. Humphrey, "Nonlinear propagation applied to the improvement of resolution in diagnostic medical ultrasound," J. Acoust. Soc. Am. **101**, 143–154 (1997).

12. S. J. Kirkpatrick, D. D. Duncan, and E. M. Wells-Gray, "Detrimental effects of speckle-pixel size matching in laser speckle contrast imaging," Opt. Lett. **33**, 2886–2888 (2008).

13. S. M. Bentzen, "Evaluation of the spatial resolution of a CT scanner by direct analysis of the edge response function," Med. Phys. **10**, 579–581 (1983).

14. J. Li, G. Ku, and L. V. Wang, "Ultrasound-modulated optical tomography of biological tissue by use of contrast of laser speckles," Appl. Opt. **41**, 6030–6035 (2002).